

A new test of the weak equivalence principle on the galaxy level based on observations of binary neutron star merger GW170817

Lulu Yao ¹, Zonghua Zhao ¹, Yu Han ¹, Jingbo Wang ¹, Tong Liu ², Molin Liu ¹★

¹ *Institute for Gravitation and Astrophysics, College of Physics and Electronic Engineering, Xinyang Normal University, Xinyang 464000, P. R. C.*

² *Department of Astronomy, Xiamen University, Xiamen, Fujian 361005, P. R. China*

Accepted XXX. Received YYY; in original form ZZZ

ABSTRACT

Because the binary neutron star (BNS) merger GW170817 and its electromagnetic (EM) counterparts were successfully detected, there is a chance to explore the joint effect of the host galaxy and the Milky Way on the weak equivalence principle (WEP) test by the gravitational-waves (GWs) and photons. In this paper, a new test of WEP is presented by modelling each galaxy composed by the Navarro-Frenk-White (NFW) halos and the Hernquist stellar. It is found that the WEP test is significantly enhanced by the joint action of the Milky Way and the NGC 4993. The constraints on the differences of the parametrized post-Newtonian (PPN) parameter $\Delta\gamma$ is under 10^{-9} for GW170817/GRB 170817A with total mass, and is under 10^{-4} for GW170817/AT 2017gfo. Following the conservative emission time difference given by [Abbott et al. \(2017d\)](#), we can obtain that $\Delta\gamma$ for GW170817/GRB 170817A is in the range of $[-5.3 \times 10^{-9}, 2.4 \times 10^{-8}]$ which is tighter by 2 orders of magnitude than previous range $[-2.6 \times 10^{-7}, 1.2 \times 10^{-6}]$. Finally, we also consider potential impacts due to uncertainties in the halos mass of NGC 4993 and the position of AT2017gfo within it, and conclude that they do not affect our results at the order of magnitude level.

Key words: Gravitational-waves – Black hole physics – Gamma-ray bursts – Binaries

1 INTRODUCTION

On 2015 September 14 the Advanced LIGO detectors picked up the first binary black hole (BBH) coalescence GW150914 and started a new era of observational gravitational-wave (GW) astronomy (see [Abbott et al. 2016](#)). Meanwhile, it is believed that besides GWs the coalescence of a binary neutron star (BNS) system is expected to produce multiple electromagnetic (EM) signatures in different timescales (e.g. [Nakar 2007](#); [Metzger 2012](#)). For a long time, people have been trying to look for the EM partners of GW, but there was no well accepted result except some possible events such as GBM transient 150914 (see [Connaughton et al. 2016](#)), until it had a big breakthrough after the detection of the GW signal GW170817, which was recorded by the LIGO/Virgo (LIV) GW observatory network on 2017 August 17, 12:41:04 UTC. The later analysis showed GW170817 was consistent with a BNS inspiral and merger by [Abbott et al. \(2017a\)](#). Then GW170817 skymap was released by LIGO/Virgo and thus drove an intensive multi-messenger campaign covering whole EM spectrum to search for the counter-

parts by [Abbott et al. \(2017b\)](#). Independently, a gamma-ray signal, classified as a short gamma-ray burst (sGRB), GRB 170817A, coincident in time and sky location with GW170817 was detected using the Fermi Gamma-ray Burst Monitor (GBM) by [Goldstein et al. \(2017\)](#) and the International Gamma-Ray Astrophysics Laboratory (INTEGRAL) by [Savchenko et al. \(2017\)](#). Beyond the sGRB, multiple independent surveys across the EM spectrum were launched in search of a counterpart. An optical counterpart (OT), Swope Supernova Survey 2017a (SSS17a, later with the IAU identification of AT 2017gfo), was first discovered using the One-Meter Two Hemisphere (1M2H) team in the optical less than 11 hours after merger, associated with NGC 4993 by [Coulter et al. \(2017\)](#), a nearby early-type E/S0 galaxy. Five other teams made independent detections of the same optical transient and host galaxy all within about one hour and reported their results of one another within about five hours including DLT40 ([Yang et al. 2017](#)), VISTA ([Tanvir et al. 2017](#)), MASTER ([Lipunov et al. 2017](#)), DECam ([Soares-Santos et al 2017](#)) and Las Cumbres ([Arcavi et al. 2017](#)). However, it should be mentioned that the statement above about the discovery of EM counterpart of GW170817 is not sufficiently convincing,

★ E-mail address: mlliu@xynu.edu.cn

and about the complete counterpart research of GW170817 one can see the review by [Abbott et al. \(2017b\)](#).

On the other hand, more and more attention has been paid to the researches of testing fundamental physics theory through the observations of high energy astronomical events (HEAE) ([Will 2014, 2006](#)). In particular, one famous scheme is testing the weak equivalence principle (WEP) by the comparison of difference waves in HEAE. The first pioneer was the test between photons and neutrinos in the supernova SN1987A in the Large Magellanic Cloud by [Longo \(1988\)](#); [Krauss et al. \(1988\)](#). More recently, such schemes have sprung up in physics and astronomy, and mainly focuses on the cosmic transients such as GRBs (e.g. [Gao et al. 2015](#); [Zhang 2016](#)), FRBs (e.g. [Wei et al. 2015](#); [Tingay & Kaplan 2016](#)), blazar flares (e.g. [Wei et al. 2016](#); [Wang et al. 2016](#)) and GW event of GW150914 (e.g. [Wu et al. 2016](#); [Kahya & Desai 2016](#); [Liu et al. 2017](#)) and so on. After the BNS merger GW170817 and its multiple EM signatures were observed by various astronomical observatories, some works have presented tests of the WEP and produced constraints on the PPN parameters (e.g. [Abbott et al. 2017d](#); [Wang et al. 2017](#); [Wei et al. 2017](#)). [Abbott et al. \(2017d\)](#) constrained on the deviation of the speed of gravity, and on violations of Lorentz invariance and the equivalence principle are presented by the observed temporal offset, the distance to source, and the assumed emission time difference, in which the bound on the difference of $\gamma_{\text{GW}} - \gamma_{\text{EM}}$ was given in the range of $[-2.6 \times 10^{-7}, 1.2 \times 10^{-6}]$. The simultaneous emission of GWs and photons was assumed by [Wang et al. \(2017\)](#), the difference of $\gamma_{\text{GW}} - \gamma_{\text{EM}}$ is under the limit of $\Delta\gamma \leq 10^{-7}$, which could be improved to 4×10^{-9} by considering the potential fluctuations from the large scale structure (see [Wang et al. 2017](#); [Nusser 2016](#)). Meanwhile, [Wei et al. \(2017\)](#) considered a Keplerian potential $\Phi = -GM/r$ for two structures, one is the Milky Way and the other is the Virgo Cluster. The case of the Milky Way adopted a total mass $6 \times 10^{11} M_{\odot}$ and found $|\Delta\gamma| < 5.9 \times 10^{-8}$ for GW170817/GRB 170817A and $|\Delta\gamma| < 1.4 \times 10^{-3}$ for GW170817/macronova. And the case of Virgo Cluster chose a total mass $1.2 \times 10^{15} M_{\odot}$ and found tighter results, i.e. $|\Delta\gamma| < 9.2 \times 10^{-11}$ for GW170817/GRB 170817A and $|\Delta\gamma| < 2.1 \times 10^{-6}$ for GW170817/macronova. It is known that Virgo Cluster is a cluster and is comprised approximately 1300 (and possibly up to 2000) member galaxies. Hence it is very larger more than the Milky Way or the NGC 4993. Here, we only focus on the scale range of enclosed mass on the level of galaxy rather than a cluster.

Meanwhile, it is known that the observer is located in our Milky Way and the source is located in host galaxy NGC 4993. For a long time, the research on the WEP has mainly focused on the gravitational potential of the Milky Way (e.g. [Abbott et al. 2017d](#); [Wang et al. 2017](#); [Wei et al. 2017](#)), while the influence of the host galaxy on the propagation of particle has been neglected because there are many uncertainties in host galaxies, such as the localization of progenitor. Fortunately, multi-messenger observations for the BNS merger GW170817, particularly in the optical counterpart AT 2017gfo, confirmed that a source was associated with NGC 4993 at a distance of 40Mpc and the merger was localized to be at a projected distance of 2 kpc away from the galaxy's center where the galactic model for NGC 4993 is presented. Motivated by these works, we focus on the

host galaxy on the test of WEP in BNS merger GW170817 through the combined profiles of the NFW halo and the Hernquist stellar, and try to estimate quantitatively the influence of the angle offset of the transient and the halo mass of NGC 4993 on these tests.

The outline of this paper is as followings. In section 2, we present a computable galactic model in the Milky Way and the NGC 4993. In section 3, we calculate the PPN parameter difference and give the WEP test between GW170817 and the EM counterparts. The section 4 is the conclusion.

2 MODEL INCLUDING THE JOINT ACTION OF THE MILKY WAY AND THE NGC 4993

The gravitational potential driving waves travelling in the interstellar space could be divided into three parts (see [Gao et al. 2015](#)): the gravitational potential of our galaxy Φ_{mw} , a flat background intergalactic potential Φ_{ig} between our galaxy and the host galaxy/cluster of the transient, the potential of the host galaxy/cluster Φ_{host} . However, Φ_{ig} and Φ_{host} are usually neglected in the WEP tests, and the main reason was the comparative lack of observations of the source. After the observation of GW170817 was detected by LIGO's Hanford detector as a single detector trigger, a full three detector localisation became available within a few hours, thus providing a reasonably small region to search. These observations drove the global efforts on the joint detection of the EM counterparts of GW170817 from a single source. Then the sGRB of GRB 170817A and an optical transient AT 2017gfo were found in the host galaxy NGC 4993 after the GW signal GW170817. Meanwhile, the source was detected and appeared in the X-ray, ultraviolet, optical, infrared, and radio bands over hours, days and weeks (see [Abbott et al. 2017b](#)). This first successful global joint detections of GW and EM radiations from a single source marks a new era in multi-messenger and time-domain astronomy, and presents a large number of important observations about the astronomical event including the host galaxy NGC 4993. Therefore, these observations provide us a good chance to use the host galaxy to test the WEP. Meanwhile, the constraint on the immediate progenitor of GW170817 from its actual formation at the time of the second SN to the final merger was presented by [Abbott et al. \(2017c\)](#). In this section we follow these observations and try to build a computable galactic model to calculate the Shapiro time of the travelling waves from the transient location to our Earth.

2.1 The travelling path of waves from the merge position

The optical transient AT 2017gfo observed by the 1M2H team using the 1 m Swope Telescope shows that the progenitor of GW170817 *S* is very likely located in NGC 4993. The geometries of the related various points including the transient source (point *S*), the centers of the Milky Way (point *G*) and the NGC 4993 (point *N*), our Earth (point *O*) are illustrated in the equatorial coordinate system (ECS) by Figure 1, and in the polar coordinate system (PCS) by Figure 2. In the two coordinate systems, the origins of ECS is our Earth and the origins of PCS is the center of the Milky Way.

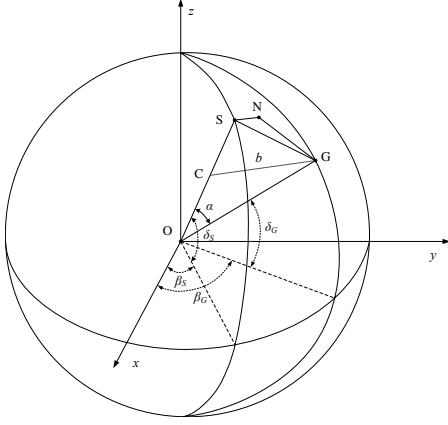


Figure 1. The localizations of the center of the Milky Way (point G) (β_G, δ_G), the merge position (point S) (β_S, δ_S) and the center of NGC 4993 (point N) (β_N, δ_N) in the equatorial coordinate system with our Earth (point O) as the origin.

Table 1. The coordinates of AT 2017gfo, the centers of NGC 4993 and Milky Way in the Equatorial coordinate system.

Object	R.A.	Decl.	References
NGC 4993	13:09:47.7	-23:23:01	Coulter et al. (2017)
AT 2017gfo	13:09:48.085	-23:22:53.343	Coulter et al. (2017)
Milky Way	17:45:40.04	-29:00:28.1	Gillessen et al. (2009)

The ECS coordinates of the transient source, the centers of the Milky Way and the NGC 4993 are listed in Table 1 by using J2000.0 (see Gillessen et al. 2009), as well as their literatures. The impact parameter b , denoted by the line GC in Figure 1, is determined by the distance from the center of the Milky Way to the travel path of messengers (see Misner et al. 1973). Meanwhile, the source was reported to be offset from the center of NGC 4993 by a projected distance of about $10''$ (e.g. Abbott et al. 2017c; Coulter et al. 2017; Levan et al. 2017; Haggard et al. 2017; Kasliwal et al. 2017). Therefore the positions of the merger and the center of NGC 4993 are not same. Meanwhile, based on the observations and analyses of the galactic environment of NGC 4993 by Hubble Space Telescope (HST) and Chandra imaging, combined with Very Large Telescope MUSE integral field spectroscopy, the binary may lie in front of the bulk of the host galaxy due to the absence of interstellar medium (ISM) absorption in the counterpart spectrum (see Levan et al. 2017).

It is known that the radius of celestial sphere has no influence on the actual viewing angle (see angle α in Figure 1) in the ECS. We hence assume the distance from our Earth to the center of the Milky Way as the radius. It approximately equals the distance from our Sun to the Galactic center, i.e. $OG \approx r_G = 8.3$ kpc. Meanwhile, the three-dimensional Cartesian coordinate system (x, y, z) could help us to find the quantitative relationship in $\triangle OSG$. Therefore, the impact parameter b and the viewing angle α should satisfy formula

$$b = SG \left(1 - \frac{SG^2}{4r_G^2} \right)^{1/2}, \quad \cos \alpha = 1 - \frac{1}{2} \left(\frac{SG}{r_G} \right)^2. \quad (1)$$

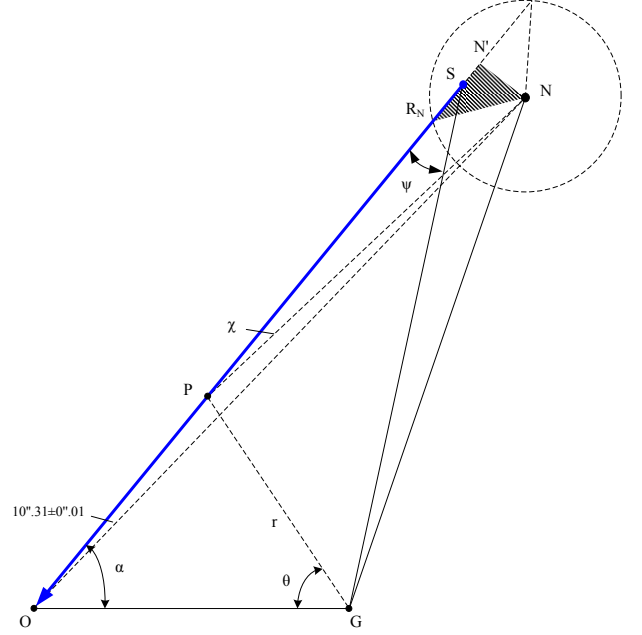


Figure 2. The travel path (blue line) of waves from the merge position (point S) to our Earth (point O) in polar coordinate system with the center of the Milky Way (point G) as the origin.

Then on the spherical surface with the radius r_G , the distance between two points can be given by

$$|SG| = \left[(x_S - x_G)^2 + (y_S - y_G)^2 + (z_S - z_G)^2 \right]^{1/2}. \quad (2)$$

The coordinates of S and G are given by (x_S, y_S, z_S) and (x_G, y_G, z_G)

$$x_S = r_G \cos \delta_S \cos \beta_S; \quad x_G = r_G \cos \delta_G \cos \beta_G; \quad (3)$$

$$y_S = r_G \cos \delta_S \sin \beta_S; \quad y_G = r_G \cos \delta_G \sin \beta_G; \quad (4)$$

$$z_S = r_G \sin \delta_S; \quad z_G = r_G \sin \delta_G, \quad (5)$$

where r_G is assumed the radius of celestial sphere. Substituting SG (2) into Eq.(1), we can get the angle α between the line on sight OS and the line from Earth to our galactic center OG . Therefore, a key trigonometric function relation associated with the angles of declination and right ascension is obtained as

$$\cos \alpha = \sin \delta_S \sin \delta_G + \cos \delta_S \cos \delta_G \cos \Delta\beta, \quad (6)$$

where $\Delta\beta = |\beta_S - \beta_G|$ is the difference between β_S and β_G . Substituting the coordinates of points S and G into Eq.(6), we can get $\alpha \approx 61.28^\circ$. Meanwhile, the impact parameter b can be finally rewritten as

$$b^2 = r_G^2 \left[1 - (\sin \delta_S \sin \delta_G + \cos \delta_S \cos \delta_G \cos \Delta\beta)^2 \right], \quad (7)$$

which is widely used in the scattering problems of galactic potential (e.g. Gao et al. 2015; Liu et al. 2017).

Then we turn to find the path of the waves travelling between the merge position and the Milky Way. In the polar coordinate system (r, θ) (see Figure 2), we consider the geometrical plane consisting of our Earth, the galactic center of the Milky Way and the merge position. At the initial time of travelling, the waves are located at point S (r_S, θ_S) and

the coordinates should satisfy following formulae

$$r_S^2 = d^2 + r_G^2 - 2r_G d \cos \alpha, \quad (8)$$

$$d^2 = r_S^2 + r_G^2 - 2r_G r_S \cos \theta_S, \quad (9)$$

where $r_S = GS$ is the distance from merge position to the center of the Milky Way, $d = OS$ is the distance from merge position to our Earth. In this way, We can obtain other angles of $\psi = 0.01^\circ$ and $\theta_S = 118.71^\circ$ in $\triangle SOG$ at the initial time of wave's travelling. The path of waves from the source (r_S, θ_S) to the final receiver ($r_G, 0^\circ$) is illustrated in Figure 2, as well as the relevant parameters. The path can give us one condition of that the angle α should be unchanged during propagation, even for a dynamical point S . Therefore, for any test point P with the coordinate (r, θ) , the angle α should satisfy the following formula

$$\cos \alpha = \frac{OP^2 + r_G^2 - r^2}{2r_G \cdot OP}. \quad (10)$$

Substituting the cosine function of angle α at the beginning travelling time in Eq.(8) into above formula (10), we can get a dynamic distance from our Earth to any position P during waves travelling shown by,

$$OP = \frac{1}{2d} \left[\zeta \pm \sqrt{\zeta^2 + 4d^2 (r^2 - r_G^2)} \right], \quad (11)$$

with $\zeta = d^2 - r_S^2 + r_G^2$. Here we keep the sign “+” in front of the square root. The joint conditions of waves propagating requires that at the initial moment of $r \rightarrow r_G$ the condition of $OP \rightarrow 0$ must be satisfied, and at the terminal moment of $r \rightarrow r_S$ the condition of $OP \rightarrow d$ also must be satisfied. The path OP in Eq.(11) with sign “+” is the path which can define the propagation of waves from the merge position to the Earth O (see Figure 2).

2.2 The gravitational potential by the joint action of the Milky Way and the NGC 4993

In this subsection, we use the structure obtained to build up a new combined gravitational potential in the galaxies of the Milky Way and the NGC 4993. Two kinds of enclosed masses are considered, one is the stellar mass and the other is the dark matter (DM) halos. The former is described using Hernquist profile in a bulge model given by Hernquist (1990), and the latter is described using the Navarro-Frenk-White (NFW) profile given by Navarro et al. (1996) in a DM model. These two kinds of profiles are analytic expressions for the distribution of the mass composition of galaxies, and are extensively applied to the dynamics of galaxies and the effect of a merger driven model for galaxy evolution.

We first give the gravitational potential of the stellar component in two galaxies of the Milky Way and the NGC 4993. The Hernquist profile of single mass source has a density distribution shown below as

$$\rho_s(r) = \frac{M_s a_b}{2\pi r (r + a_b)^3}, \quad (12)$$

where M_s is the total stellar mass and a_b is a scale length. The gravitational potential is given by

$$\Phi_{\text{stellar}}(r) = -\frac{GM_s}{r + a_b}. \quad (13)$$

Table 2. The DM halos parameters obtained through NFW model.

NFW Parameters	Milky Way	NGC 4993
median $r_{200}(\text{kpc})$	208	282
concentration parameter c_{200}	6.5	5.9
density parameter $\rho_0 (10^{-3} M_\odot \text{pc}^{-3})$	2.0	1.6
scale radius R_s (kpc)	32	48

The stellar mass of the Milky Way is $6.4 \times 10^{10} M_\odot$ given by McMillan (2011), and the stellar mass of NGC 4993 is $6.2 \times 10^{10} M_\odot$ provided by Lim et al. (2017). The bulge scale length is 0.5 kpc for our galaxy given by Sofue et al. (2009). The bulge scale length of host galaxy NGC 4993 is about 0.55 times of the half light radius R_{eff} (see Hernquist 1990), which was observed recently as $15.''5 \pm 1.''5$, corresponding to 3.0 kpc offset for a distance of 40 Mpc, by using HST measurements by Hjorth et al. (2017).

Then we turn to present the gravitational potential of the DM halos in two galaxies. The DM halo is described by the NFW profile, and the density distribution of halos in single mass source is thus presented by the formula,

$$\rho_{\text{DM}}(r) = \frac{\rho_0 R_s}{r} \left(1 + \frac{r}{R_s} \right)^{-2}, \quad (14)$$

where ρ_0 is the density parameter and R_s is the scale radius defined by $R_s = R_{200}/c_{200}$. R_{200} is the position that the enclosed density is 200 times the universe's critical density. c_{200} is the concentration parameter could be obtained via the empirical expression given by Duffy et al. (2008)

$$\log_{10} c_{200} = (0.76 \pm_{-0.01}^{0.01}) + (-0.10 \pm_{-0.01}^{0.01}) \log_{10} \left(\frac{M_{200}}{M_{\text{pivot}}} \right), \quad (15)$$

where the median halos mass $M_{\text{pivot}} = 2 \times 10^{12} h^{-1} M_\odot$. Based on the report from Planck Collaboration (2016) the median value for the Hubble parameter is $h = 0.679$. The DM halos mass of the Milky Way is adopted as $0.9_{-0.3}^{+0.4} \times 10^{12} M_\odot$ which was obtained by using 4664 blue horizontal branch stars given by Kafle et al. (2012). For the DM halos mass of NGC 4993 is adopted as $(10^{12.2} h^{-1}) M_\odot$ which was obtained by using the 2MASS Redshift Survey (2MRS) in the low redshift universe given by Lim et al. (2017). The parameters ($\rho_0, R_s, R_{200}, c_{200}$) thus can be obtained through modeling NFW halos, which are listed in Table 2. Then, the gravitational potential of NFW halos is given by

$$\Phi_{\text{DM}}(r) = -\frac{4\pi G \rho_0 R_s^3}{r} \ln \left(1 + \frac{r}{R_s} \right). \quad (16)$$

By considering above two main components of potential for the stellar and the DM halos, we can present the total gravitational potential Φ_{total} consisted of our galaxy and the host galaxy,

$$\Phi_{\text{total}} = \Phi_{\text{mw}} + \Phi_{\text{host}}, \quad (17)$$

where the potential Φ_{mw} of Milky Way (or Φ_{host} of NGC 4993), composed by the Hernquist stellar sector Φ_{s1} (or Φ_{s2} of NGC 4993) yielded to Eq.(13) and the NFW halos sector Φ_{D1} (or Φ_{D2} of NGC 4993) yielded to Eq.(16), is written as

$$\Phi_{\text{mw}} = \Phi_{s1}(r) + \Phi_{D1}(r), \quad (18)$$

$$\Phi_{\text{host}} = \Phi_{s2}(\chi) + \Phi_{D2}(\chi), \quad (19)$$

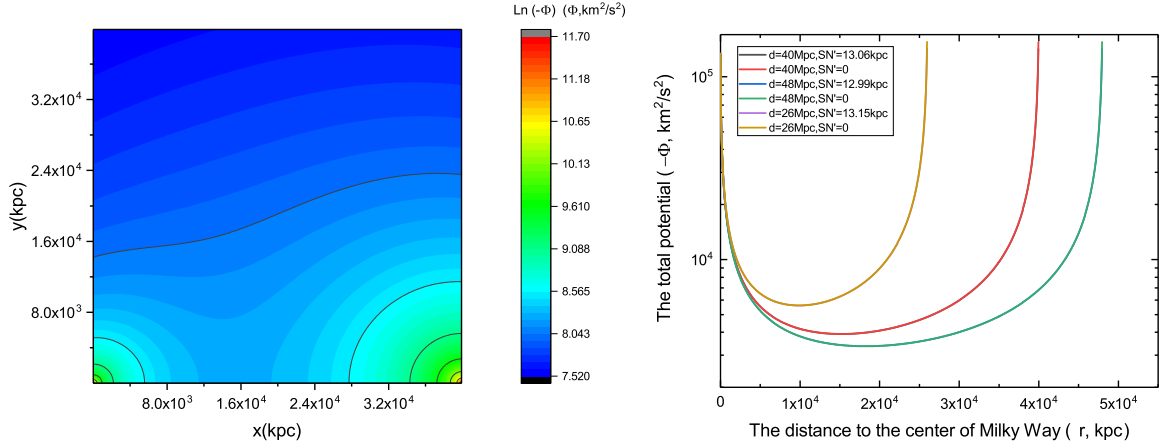


Figure 3. The left figure is the contour plots of the gravitational potential by the joint action of the Milky Way and the NGC 4993 with the median magnitude of luminosity distance $d = 40$ Mpc. The right figure is the potential along the waves path SP (see Figure 2) with the observed angle offset of $SN' \in [0, 13.06_{-0.07}^{+0.09}]$ kpc.

where $\chi(r, \theta)$ is a dynamical distance from the center of NGC 4993 to the any given point P. It should be noted that the model parameters for the Hernquist stellar both in the Milky Way and the NGC 4993 are given below Eq.(13), the parameters of the NFW halos are listed in Table 2. If one want the waves at point P travels along the path (see the blue line in Figure 2), one condition should be respected as

$$\chi(r, \theta) = \left[r^2 + GN^2 - 2GNr \cos(\theta_S - \theta) \right]^{1/2}, \quad (20)$$

where for the cosmic source GW170817 we have $GN \approx d$ and the angle θ_S of the merger position approximately equal to the angle $\angle NGO$ of the center of NGC 4993.

Φ_{total} (17) is illustrated in Figure 3 in which the left subgraph is the contour plots of gravitational potential at any point on the plane contained the line between the centers of two galaxies where the median magnitude of luminosity distance $d = 40$ Mpc is adopted and the magnitude of potential covers all the space. The right subgraph is the potential along the path by considering the condition (20) where the observed luminosity distance of $d = 40_{-14}^{+8}$ Mpc is adopted and the effect of observed angle offset is considered. Two subgraphs strongly suggest that the impacts of the host galaxy on the total potential should not be ignored.

2.3 The angle offset of the transient location and the large natal kick of the binary

The HST and Chandra imaging combined with Very Large Telescope MUSE integral field spectroscopy presented a lower limit on the true offset by Levan et al. (2017). The transient was located at position offset $8''.92$ N and $5''.18$ E of the host galaxy centroid, with a total projected angle offset of $\alpha_o = 10''.31 \pm 0''.01$, corresponding to 1.96 kpc offset at a 40 Mpc distance. It implies that the source was located in the region bounded by the observational angle offset (see the shaded area in Figure 2). Meanwhile, due to there is a possible large natal kick of the binary (see Abbott et al. 2017c), the source maybe be kicked outside of the gravitational grasp of the galaxy NGC 4993. The major factors affecting the WEP test come from the angle offset and the

large natal kick. We thus focus on these points and do some quantitative analyses here.

In order to illustrate these problems clearly, we turn to Figure 2 where the center of NGC 4993 is denoted by point N and its projected point on the line on sight is denoted by point N' . Because there is a projected relationship in $\triangle PNN'$, we can get a right-angle $\angle PN'N$ and the distance NP about the test position shown by

$$NP = \sqrt{N'N^2 + N'P^2}, \quad (21)$$

with $N'P = OS + N'S - OP$ and $N'N = d \sin \alpha_o$. Here, $N'N$ is the projected offset distance from the center of the galaxy, OS is the distance from the source to our Earth, OP is given by Eq.(11). Thus NP could be completely determined by the distance r from a given position to the center of our Milky Way, except for the last parametric of the distance of $N'S$ which could not be confirmed by current observations because the source location relative to its host cannot be measured along the line on sight.

We then check the distance uncertainty caused by the observed offset angle, which could be calculated quantitatively by the distance of $N'S$ inside the host galaxy NGC 4993. It is easy to find that the minimum of $N'S$ comes from the situation in which the source S is located at the projected point N' . The minimum of $N'S$ is zero. On the other side, the maximum of $N'S$ comes from the situation of that the source is located at the front outermost edge (the bulk denoted by the dash line) of the galaxy along the line on sight, i.e. the source S is located at the point R_N where $R_N N = R_N$ is the half of the galaxy diameter. By using the NASA Extragalactic Database (NED) or the ESO-LV catalogue (see Lauberts & Valentijn 1989), we can obtain the diameter of 26 kpc for NGC 4993. Therefore, we can get the minimum and the maximum of $N'S$ shown by

$$N'S|_{\min} = 0, \quad (22)$$

$$N'S|_{\max} = N'R_N = \sqrt{R_N^2 - N'N^2}. \quad (23)$$

The range of $N'S$ is thus determined by the distance d from the source S to the receiver O. Based on the luminosity distance observed by Abbott et al. (2017a), the different magnitudes of d give us the different maximum $N'S$ but they

are all about 13 kpc. Namely, the upper limit luminosity distance 48 Mpc gives the maximum of 12.99 kpc, and the lower-limit luminosity distance 26 Mpc gives the maximum of 13.15 kpc, and the median magnitude 40 Mpc gives the maximum of 13.06 kpc. Hence, we can give the distance $N'S$ in the range of $[0, 13.06^{+0.09}_{-0.07} \text{ kpc}]$ where the maximum uncertainty comes from the luminosity distance.

Then we use the formula presented by Liu et al. (2017), which were used to study the impacts on the test of WEP by the distance difference between separated detectors H1 and L1 for GW150914, to estimate quantitatively the uncertainty caused by the distance offset from the center of galaxy. Considering a perturbation $d \rightarrow d + \delta d$ along the wave path, the upper limit of γ parameter difference $\Delta\gamma$ is changed to $\Delta\gamma + \delta\Delta\gamma$ and the relative deviation is given by

$$\Delta = \left| \frac{\delta\Delta\gamma}{\Delta\gamma} \right| = \frac{1}{\log(d/b)} \frac{\delta d}{d}, \quad (24)$$

where the impact parameter b is given by Eq.(7). One can choose the parameters of $b \sim r_G \sim 8.3$ kpc, $d \sim 26$ Mpc and $\delta d \sim 13.15$ kpc to make a conservative estimation, a relative deviation thus could be obtained as $\Delta \sim 4 \times 10^{-3}$. It means that this kind of offset basically does not affect the order of magnitude of the result. Meanwhile, if we follow the precision of the observed angle offset of $\alpha_o = 10''.31 \pm 0''.01$, we find that the bias of $\pm 0''.01$ does not effect the final results at the order of magnitude level. This point is also illustrated by the right subgraph of Figure 3 where the effect of observed angle offset of $SN' \in [0, 13.06^{+0.09}_{-0.07} \text{ kpc}]$ is considered. One can find that when $d = 40$ Mpc the potentials with $SN' = 13.06$ kpc or $SN' = 0$ are highly overlapping, and the same situations also could be found in the remain kinds of $d = 48$ Mpc and $d = 26$ Mpc. It means that the influence of offset distance NN' on the potential of travelling wave is small.

Except for above observed offset angle, the second SN (SN2) kick also has a large effect on the actual distance to the final merger. According to the kinematic modeling from the SN2 to the merger (see Abbott et al. 2017c), the slingshot effect caused by the tangential SN2 kick is much more efficient than a purely radial kick to drive the binary to outer regions of the galaxy. Therefore, a large natal kick of the binary could make it merge at a greater distance. The final merger position is possible to be out of the range of galaxy for a larger SN2 kick, as long as the observed offset angle is respected. Therefore, the merger position S may be out the range of $|N'R_N|$ (see Figure 2) and the real distance R_{real} from the SN2 to the merger is simplified as follows

$$R_{\text{real}} = \tau_{\text{gwr}} V_{\text{kick}}, \quad (25)$$

where τ_{gwr} is the merger time of BNS. It was studied in many references, such as the original work about the motion of two point masses in gravitational radiation (see Peters 1964), and the first constraints on the progenitor of GW170817 at the time of the SN2. Here, in order to get the maximum uncertainty caused by SN2 kick, we choose a more looser constraint on the distance R_{real} and adopt the value of τ_{gwr} in the range of $\tau_{\text{gwr}0} \lesssim \tau_{\text{gwr}} \lesssim t_{\text{Hubble}}$ where $t_{\text{Hubble}} = 1/H_0$ with $H_0 = 100 \text{ hkm s}^{-1} \text{ Mpc}^{-1}$ is the Hubble time and $\tau_{\text{gwr}0}$ is the minimum merger time 86 Myr from the observation of PSR J0737-3039A/B in a highly relativistic orbit (e.g. Tauris et al. 2017; Kramer et al. 2006;

Breton et al. 2008; Ferdman et al. 2013). V_{kick} is the kick velocity along the radial direction, which is assumed to be unchanged after the SN2. Whereas there is ample observational evidence for large NS kicks (typically $400 \sim 500 \text{ km s}^{-1}$) in observations of young radio pulsars (e.g. Abbott et al. 2017c; Tauris et al. 2017). Therefore, the real distance of binary after the SN2 can be estimated as

$$(36 \sim 45) \text{ kpc} \lesssim R_{\text{real}} \lesssim (2.7 \sim 3.4) \times 10^3 \text{ kpc}, \quad (26)$$

which is beyond the diameter 26 kpc of the galaxy NGC 4993 (see Lauberts & Valentijn 1989). If we consider that the perturbation δd is from the distance R_{real} , we can use the formulae in Section 2.3 to estimate quantitatively the uncertainty caused by above large natal kick. The relative deviations Δ are listed in Table 3, which shows that the large natal kick of the binary does not affect the results at the order of magnitude level.

3 THE WEP TEST IN THE MILKY WAY AND THE NGC 4993 FOR THE BINARY NEUTRON STAR MERGER GW170817

After building the computable model of the galaxies, we can thus constrain the WEP through comparison of PPN parameter difference between the different waves. Following the formulae in literature (e.g. Shapiro 1964; Longo 1988; Krauss et al. 1988), the important Shapiro time delay Δt_{gra} could be obtained through the integration of gravitational potential along the path of the waves

$$\Delta t_{\text{gra}} = -\frac{1+\gamma}{c^3} \int_{r_e}^{r_o} \Phi(r) dr, \quad (27)$$

where $r_e = r_S$ and $r_o = r_G$ denote the positions of sender and receiver. Meanwhile, in order to define the waves travel along the path from the merge position to our Earth, the condition of Eq.(21) must be respected.

3.1 The constraints on the WEP test between GW170817 and GRB 170817A

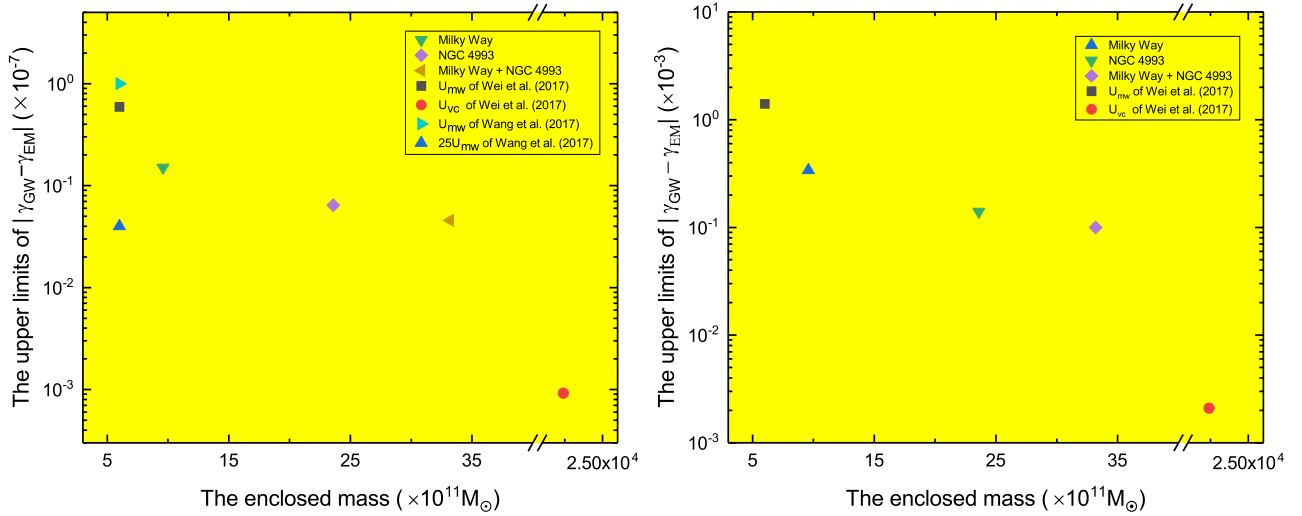
In our calculations, two counterparts of GW170817 are chosen to perform the WEP test. One is GRB 170817A observed using Fermi GBM by Goldstein et al. (2017) and the Integral by Savchenko et al. (2017), and the other is AT 2017gfo observed by 1M2H. We first study the WEP test between GW170817 and GRB 170817A. On August 17, 2017 at 12:41:06 UTC the Fermi GBM detected and triggered on the short gamma-ray burst GRB 170817A. The temporal offset between the BNS merger and the GRB is observed and shown by Abbott et al. (2017b); Goldstein et al. (2017)

$$\Delta t_1 \equiv T_{\text{GRB}} - t_c = 1.734 \pm 0.054 \text{ s}. \quad (28)$$

The maximum time delay caused by gravity comes from above observed temporal offset (28). Substituting Eq.(28) into the Shapiro time (27), we can obtain the upper limit of PPN parameter difference between GW170817 and GRB 170817A in the gravitational potentials of two galaxies, denoted by $|\Delta\gamma_1| \equiv |\gamma_{\text{GW}} - \gamma_{\text{EM}}|$ listed in Table 4. Because there is an observed angle offset, we perform our calculations by considering two cases. One is the minimum

Table 3. The relative deviations from the large natal kick within the delay time from the BNS birth to the merger.

d	V_{kick}	τ_{gwr}	δd	Δ
26 Mpc	400 km/s	t_{Hubble}	2.7 Mpc	0.01
	500 km/s	t_{Hubble}	3.4 Mpc	0.02
	400 km/s	86 Myr	36 kpc	0.0002
	500 km/s	86 Myr	45 kpc	0.0002
48 Mpc	400 km/s	t_{Hubble}	2.7 Mpc	0.006
	500 km/s	t_{Hubble}	3.4 Mpc	0.008
	400 km/s	86 Myr	36 kpc	0.00009
	500 km/s	86 Myr	45 kpc	0.0001


Figure 4. The upper limit of PPN parameter differences for two kinds comparison: GW170817/GRB 170817A (left figure) and GW170817/AT 2017gfo (right figure) where the source is conservatively assumed located at the projected point N' of the center of NGC 4993. The other results given by Wei et al. (2017); Wang et al. (2017) on the galaxy level are also listed including U_{mw} for the Milky Way and a potential $\sim 25U_{\text{mw}}$, as well as the result of U_{vc} on the cluster level.

value of $SN' = 0$ with the transient S located at the projected point N' , and the other is the maximum value of $SN' = 13.06^{+0.09}_{-0.07}$ kpc with the transient S located at the point R_N near the edge of NGC 4993.

We first consider the conservative situation of that the source is located at the projected point N' of the center of NGC 4993, which is corresponding the case of the minimum $SN' \sim 0$. It is found that the difference $|\Delta\gamma_1|$ between GW170817 and GRB 170817A is under 10^{-8} for the Milky Way by using the potential Φ_{mw} (18). It is consistent with the results given by Wei et al. (2017) through the a Keplerian potential with the total mass $\sim 6 \times 10^{11} M_{\odot}$ of the Milky Way. Meanwhile, our result is also tighter by 1 order of magnitude than that of Wang et al. (2017) through using the impact parameter of the particle paths relative to the center of the Milky Way where the total mass also was adopted as $6 \times 10^{11} M_{\odot}$. About the relevant comparisons one can refer to the left subgraph in Figure 4. We also surprisingly find that such a constraint on PPN parameter can be improved significantly by the host galaxy on the level of galaxy, which is under 10^{-9} both for Φ_{host} (19) of NGC 4993 and for Φ_{total} (17) of total mass in two galaxies. These results are listed in Table 4 (see the part of $\Delta\gamma_1$) and in Figure 4 (see the left subgraph).

Then we enlarge appropriately the hypothesis of the source to be located at the edge of galaxy, which is corre-

sponding the case of the maximum SN' . Its magnitude depends on the observed luminosity distance due to the projected angle offset. For the detailed discussions about this aspect, one can see former subsection 2.3. The results for the enclosed masse inside the three types scales, i.e. Milky Way, NGC 4993, Milky Way + NGC 4993, are also listed in Table 4. One can find that the orders of magnitude are the same as these of $SN' = 0$. Basically, when the source changes from the point N' to the point R_N near the edge of galaxy, the WEP test is unchanged for the case of the Milky Way, and becomes slight looser for the cases of NGC 4993 and NGC 4993 + Milky Way.

3.2 The constraints on the WEP test between GW170817 and AT 2017gfo

Then we turn to constrain the WEP test by comparing PPN parameter difference $\Delta\gamma_2$ between GW170817 and AT 2017gfo in the galaxies. On August 17, 2017 at 23:33 UTC the 1M2H team found a transient and fading optical source SSS17a/AT 2017gfo coincident with GW170817. AT 2017gfo is located in NGC 4993, an S0 galaxy at a distance of 40 Mpc. The precise location of GW170817 provides an opportunity to probe the nature of these cataclysmic events by combining electromagnetic and GW observations. The transient AT 2017gfo was $i = 17.057 \pm 0.018 \text{ mag}$ and did not

Table 4. The PPN parameter differences with a $10.31''$ total projected angle offset where the distance of source is adopted as 40_{-14}^{+8} Mpc for the cases of $|\Delta\gamma_1|$ and $|\Delta\gamma_2|$, and 26 Mpc for the case of $|\Delta\gamma_3|$.

Comparison Type	S located at N'	S located at R_N	Enclosed mass
GW170817/GRB170817A ($ \Delta\gamma_1 \lesssim$)	$1.5_{-0.1}^{+0.2} \times 10^{-8}$	$1.5_{-0.1}^{+0.2} \times 10^{-8}$	Milky Way
	$6.4_{-0.8}^{+0.8} \times 10^{-9}$	$6.5_{-0.8}^{+0.8} \times 10^{-9}$	NGC 4993
	$4.5_{-0.3}^{+0.3} \times 10^{-9}$	$4.6_{-0.3}^{+0.3} \times 10^{-9}$	Milky Way + NGC 4993
GW170817/AT2017gfo ($ \Delta\gamma_2 \lesssim$)	$3.4_{-0.2}^{+0.6} \times 10^{-4}$	$3.4_{-0.2}^{+0.4} \times 10^{-4}$	Milky Way
	$1.4_{-0.2}^{+0.2} \times 10^{-4}$	$1.5_{-0.2}^{+0.2} \times 10^{-4}$	NGC 4993
	$1.0_{-0.1}^{+0.1} \times 10^{-4}$	$1.0_{-0.1}^{+0.1} \times 10^{-4}$	Milky Way + NGC 4993
GW170817/GRB170817A ($\Delta\gamma_3 \gtrsim$)	-1.7×10^{-8}	-1.8×10^{-8}	Milky Way
	-7.5×10^{-9}	-7.6×10^{-9}	NGC 4993
	-5.3×10^{-9}	-5.3×10^{-9}	Milky Way + NGC 4993
GW170817/GRB170817A ($\Delta\gamma_3 \lesssim$)	8.1×10^{-8}	8.1×10^{-8}	Milky Way
	3.4×10^{-8}	3.5×10^{-8}	NGC 4993
	2.4×10^{-8}	2.4×10^{-8}	Milky Way + NGC 4993

match any known asteroid or supernova. The observations (e.g. Abbott et al. 2017b; Goldstein et al. 2017) show that the time difference between the binary merger GW170817 and AT 2017gfo was

$$\Delta t_2 \equiv T_{\text{OT}} - t_c = 10.87 \text{ hr}. \quad (29)$$

If we treat this time offset as the Shapiro time delay of the comparison of GW170817/AT 2017gfo, the upper limit of their parameter difference $|\Delta\gamma_2| \equiv |\gamma_{\text{GW}} - \gamma_{\text{EM}}|$ can be obtained through the similar calculations in former subsection 3.1. The results listed in Table 4 (see the part of $\Delta\gamma_2$) and in Figure 4 (see the right subgraph) can be obtained by the enclosed masse consisted of the Hernquist stellar describe by formula (13) and the NFW halos describe by formula (16).

For the conservative case with the minimum SN' , the differences of $|\Delta\gamma_2|$ between GW170817 and AT 2017gfo are all under 10^{-4} for the three types galaxy scales, i.e. Milky Way, NGC 4993, Milky Way + NGC 4993. It is tighter distinctly by 1 order of magnitude than the results in usual Keplerian potential for GW170817/AT 2017gfo given by Wei et al. (2017) (see the right subgraph in Figure 4). Meanwhile, when comparing with the comparison of GW170817/GRB 170817A in the former subsection 3.1, one can find the results of GW170817/AT 2017gfo are looser by 4 or 5 orders of magnitude for three types scales on the level of galaxy. It suggests that with increasing Shapiro time delay the upper limit of PPN parameter difference will increase, and the constraints on the WEP thus become looser. Meanwhile, the results of $|\Delta\gamma_2|$ for the maximum distance of SN' are also listed in Table 4 and in Figure 4. It is found that the change of the location of the source from the point N' near the center to the point R_N near the edge of NGC 4993 does not influence the orders of magnitude in the three scales. Basically, the angle offset does not impact the magnitude of the PPN differences of Φ_{mw} (18) in the Milky Way.

3.3 The constraints on PPN parameter with a non-zero emission time difference

A joint research group consisting of LIGO, Virgo, Fermi GBM and INTEGRAL (LVFI) (see Abbott et al. 2017d) have presented the implications of GW170817 and its EM counterparts on the fundamental physics including the speed of GW, the Lorentz invariance violation limits, the test of the WEP and so on, through the temporal offset (28) measured

between GW170817 and GRB170817A (see Abbott et al. 2017a) with a lower-limit luminosity distance 26 Mpc. In their WEP test, a conservative bound on $\gamma_{\text{EM}} - \gamma_{\text{GW}}$ was determined by considering the effect of the Milky Way outside a sphere of 100 kpc and by using a Keplerian potential with the mass of $2.5 \times 10^{11} M_{\odot}$.

We use $\Delta t_3 \equiv t_{\text{EM}} - t_{\text{GW}}$ to denote the upper and lower limits on the difference of the travel time between GW170817 and GRB170817A. Here t_{EM} and t_{GW} are the travelling times of EM and GWs respectively. If the travelling time difference is positive, i.e. $\Delta t_3 > 0$, the EM will propagate faster than GW. On the contrary, the difference $\Delta t_3 < 0$ means the EM will propagate slower than GW. Then we can turn to the upper limit of the travel time difference Δt_3 which could be obtained by an assumption that the first photons are emitted at the emission time of the peak of the GW signal. Therefore, this kind of assumption attributes the entire temporal offset to faster travel by the GW signal and an upper bound on the relative speed difference $\Delta v/\nu_{\text{EM}}$ is 7×10^{-16} (see Abbott et al. 2017d). Based on former formula (27), this kind of upper limit of Δt_3 give us a lower bound on the PPN parameter difference $\Delta\gamma_3 \equiv \gamma_{\text{GW}} - \gamma_{\text{EM}}$.

Following the conservative time interval given by Abbott et al. (2017d), the lower bound of the difference $\Delta\gamma_3$ are thus obtained in Table 4 (see the part of $\Delta\gamma_3$) and in Figure 5. For the case of the minimum SN' , the lower bound of $\Delta\gamma_3$ is -10^{-8} for Φ_{mw} (18) in Milky Way, -10^{-9} for Φ_{host} (19) in NGC 4993 and Φ_{total} (17) in Milky Way + NGC 4993, in which the “-” means the EM waves are faster than GWs (see Abbott et al. 2017d). When comparing with the results of $\Delta\gamma_3 \gtrsim -2.6 \times 10^{-7}$ given by Abbott et al. (2017d), one can find that the result of Milky Way is tighter by 1 order of magnitude, and the results of NGC 4993 and NGC 4993 + Milky Way are all tighter by 2 orders of magnitude. The WEP test is significantly enhanced through the enclosed mass composed by NFW halos and Hernquist stellar with the effect of the host galaxy. Meanwhile, the results of the maximum SN' are also listed in Table 4 and have the same orders of magnitude as these of the case of the minimum SN' .

Then we turn to check the lower limit of the travel time difference Δt_3 which could be obtained by another assumption that two signals were emitted at times differing by more than $(+1.734 \pm 0.054)$ s with the faster EM signal making up some of the difference. Here we choose a prudent calcula-

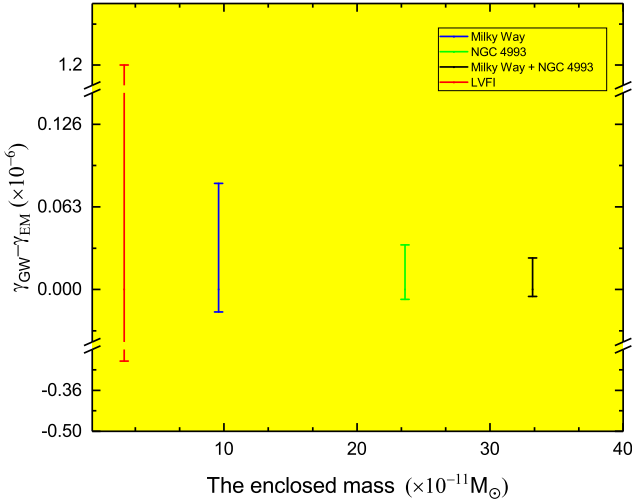


Figure 5. The interval of the PPN parameter difference between GWs and EM for the Hernquist stellar mass (green), the NFW halos (blue) and the total mass (black) where the result (red) of Abbott et al. (2017d) is also listed.

tion strategy and use the selection of that the SGRB signal was emitted 10 s after the GW signal, given by the joint research group: LIGO, Virgo, Fermi GBM and INTEGRAL (see Abbott et al. 2017d). Therefore, we can get the lower limit of the travel time difference $\Delta t_3 = -(10 - 1.734 \pm 0.054)$ s and an upper bound on the relative speed difference $\Delta v/v_{\text{EM}}$ is -3×10^{-15} . Substituting above time delay Δt_3 into the Shapiro time delay (27), we can get the upper bound on the PPN parameter difference. The cases of the minimum and the maximum SN' are all listed in Table 4, the lower limit of travel time difference Δt_3 gives the same upper bound as 10^{-8} for Milky Way, NGC 4993, and Milky Way + NGC 4993, which is also tighter by 2 orders of magnitude than the bound 1.2×10^{-6} given by Abbott et al. (2017d) (see Figure 5).

3.4 The influence of the halo mass of NGC 4993 with a 0.2 dex scatter on the WEP test

Then we discuss the rationality of the selection about the halo mass of NGC 4993. It is known that in 2MRS, one cross-identification of NGC 4993 is 2MASX J13094770-2323017 by Huchra et al. (2012). Meanwhile, using galaxy systems as a proxy of the halos population is the important group finder. One halo based group finder was proposed by Yang et al. (2005) and has been extensively tested using mock galaxies from simulations and found to perform much better in identifying poor systems. Then Lim et al. (2017) applied 2MRS to construct the group catalogs in the low redshift universe by used a improved halo based group finder. In Lim's catalogs, the 2MRS(M) of Low Redshift Group Catalog was given by using the Proxy-M to estimate halo masses to the galaxies that have spectroscopic redshifts. In 2MRS(M) one can find that NGC 4993 is in the group 4940 which has only 2 galaxies and is obviously a poor system. Furthermore, the group 4940 is inside the region of completeness for a given halo mass, and thus can assign halo mass by abundance matching. In Figure 6 we draw 5 sub-figures to illustrate

how the related groups are dynamical in three kinds of catalogs: the 2MRS Group Catalog provided by Lu et al. (2016), the 2MRS(L) and the 2MRS(M) in Low Redshift Group Catalog. It is easy to find that with the member number decreasing, the group will become a poor system and the properties of the group would be close to that of galaxies. Based on these situations, we can thus use the halo mass of the poor system to identify that of galaxy NGC 4993. Meanwhile, this kind of choice $10^{12.2}/h M_{\odot}$ also could be found in the constraints on the progenitor of GW170817 at the time of the second supernova (see Abbott et al. 2017c).

In the catalog of 2MRS(M) (see Lim et al. 2017), the halo masses assigned by the group finder are un-biased with respect to the true halo masses, but have a typical uncertainty of ~ 0.2 dex. Then we discuss how much uncertainty is created in the result of $\Delta\gamma$ by the scatter with ~ 0.2 dex. The parameters of the NFW halos with the maximum and the minimum halo mass of NGC 4993 are listed in Table 6. Based on the new parameters we recalculate our results of $|\Delta\gamma_1|$, $|\Delta\gamma_2|$, and the conservative lower and upper bounds of $\Delta\gamma_3$. The results are listed in Table 5 where the maximum halo mass is $10^{12.4} h^{-1} M_{\odot}$ and the minimum halo mass is $10^{12.0} h^{-1} M_{\odot}$.

It is found that when comparing with the results of the median halo mass $10^{12.2}/h M_{\odot}$ for NGC 4993 (see Table 4), three tests are changed slightly, and the remain tests all stayed the same order of magnitude. The changed three tests are given as followings. Two are from the upper limits of $|\Delta\gamma_2|$ with the maximum halo mass for NGC 4993 and Milky Way + NGC 4993, which are tighter by 1 order of magnitude than that of the median halo mass. It means that the test of long time delay is sensitive to the halo mass. The last one is from the lower limit of $|\Delta\gamma_3|$ with the minimum halo mass for NGC 4993, which is looser by 1 order of magnitude than that of the median halo mass. Except for these cases, the results are consistent with each other in the median mass, the minimum mass and the maximum mass for the halo of NGC 4993. Therefore, the 0.2 dex uncertainty caused by the halo mass scatter of NGC 4993 does not affect the orders of magnitude of the result basically.

4 CONCLUSION

In this paper, we present a new WEP test for the BNS merger GW170817 by considering the contribution from the host galaxy based on the observations of the NGC 4993 (see Abbott et al. 2017c; Coulter et al. 2017). The total potential given here can be used to describe the waves propagating between the Milky Way and the NGC 4993. It should be noted that although the result 10^{-11} of Wei et al. (2017) for Virgo Cluster is tighter about 2 orders of magnitude than our result, the methods of the scale range of enclosed mass are completely different because that Virgo Cluster is a cluster of galaxies, and is very larger more than the simple galaxy of the Milky Way or the NGC 4993. Our calculation here is only stay on the level of galaxy rather than cluster, i.e. Milky Way or NGC 4993. Therefore, the size of Virgo Cluster is outside the scale range of our calculation which only focuses on galaxy. We then summarize what have been achieved.

Firstly, unlike previous methods given by Abbott et al. (2017d); Wang et al. (2017); Wei et al. (2017), we present a

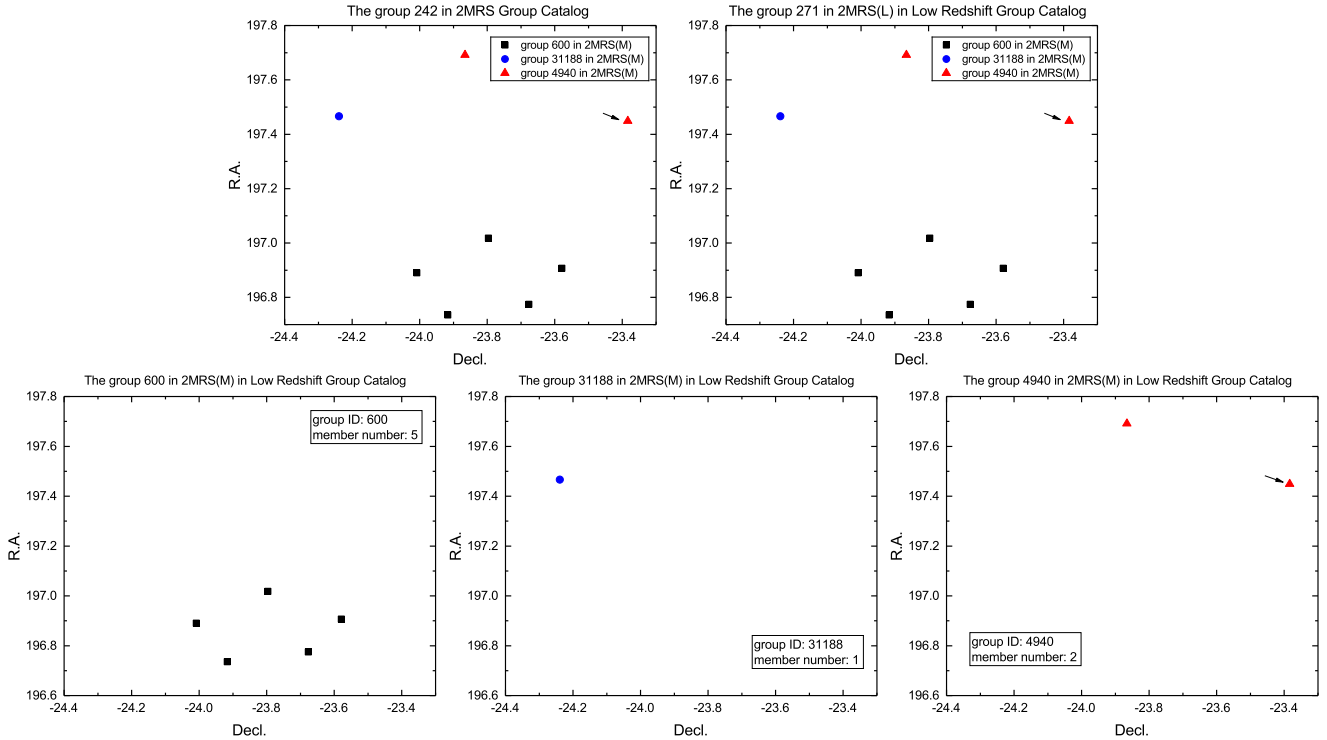


Figure 6. The evolution of NGC 4993 (indicated by the arrows) in various group catalogs. The group constituted by eight galaxies did not change either in 2MRS Group Catalog (top left, group 242 of 2MRS) or in 2MRS(L) in Low Redshift Group Catalog (top right, group 271 of 2MRS(L)). However, the group 271 of 2MRS(L) was split into three small groups in 2MRS(M) in Low Redshift Group Catalog: the group 600 (bottom left), the group 31188 (bottom middle) and the group 4940 (bottom right). With the group catalog reinforced and the number members decreased, the group thus can give more reliable information about the galaxy, particularly for the groups containing one member or a small number of members.

Table 5. The PPN parameters differences contained the halo mass of NGC 4993 with 0.2 dex scatter.

Comparison Type	Maximum halo mass	Minimum halo mass	Enclosed mass
GW170817/GRB170817A ($ \Delta\gamma_1 \lesssim$)	$1.5^{+0.2}_{-0.1} \times 10^{-8}$	$1.5^{+0.2}_{-0.1} \times 10^{-8}$	Milky Way
	$4.2^{+0.5}_{-0.2} \times 10^{-9}$	$9.8^{+0.3}_{-0.5} \times 10^{-9}$	NGC 4993
	$3.3^{+0.4}_{-0.2} \times 10^{-9}$	$6.0^{+0.7}_{-0.3} \times 10^{-9}$	Milky Way + NGC 4993
GW170817/AT2017gfo ($ \Delta\gamma_2 \lesssim$)	$3.4^{+0.4}_{-0.2} \times 10^{-4}$	$3.4^{+0.4}_{-0.2} \times 10^{-4}$	Milky Way
	$9.5^{+0.5}_{-0.5} \times 10^{-5}$	$2.2^{+0.2}_{-0.1} \times 10^{-4}$	NGC 4993
	$7.5^{+1.0}_{-0.4} \times 10^{-5}$	$1.3^{+0.2}_{-0.1} \times 10^{-4}$	Milky Way + NGC 4993
GW170817/GRB170817A ($\Delta\gamma_3 \gtrsim$)	-1.8×10^{-8}	-1.8×10^{-8}	Milky Way
	-4.9×10^{-9}	-1.1×10^{-8}	NGC 4993
	-3.9×10^{-9}	-6.9×10^{-9}	Milky Way + NGC 4993
GW170817/GRB170817A ($\Delta\gamma_3 \lesssim$)	8.1×10^{-8}	8.1×10^{-8}	Milky Way
	2.3×10^{-8}	5.2×10^{-8}	NGC 4993
	1.8×10^{-8}	3.2×10^{-8}	Milky Way + NGC 4993

Table 6. The NFW halos parameters of NGC 4993 with a 0.2 dex scatter.

NFW Parameters	Upper limit	Lower limit
halo mass M_{DM} (M_{\odot}/h)	$10^{12.4}$	$10^{12.0}$
median r_{200} (kpc)	328	243
concentration parameter c_{200}	5.6	6.2
density parameter ρ_0 ($10^{-3} M_{\odot} \text{pc}^{-3}$)	1.5	1.8
scale radius R_s (kpc)	58	39

new scheme which considers the influence of host galaxy on these test waves. A new combined gravitational potential is

given in the Milky Way and NGC 4993. The PPN parameter differences between photon and graviton thus are obtained. The enclosed mass of the galaxies consists of Hernquist stellar mass and NFW halos mass, in which the Hernquist stellar masses are chosen as $6.4 \times 10^{10} M_{\odot}$ for the Milky Way with the bulge of 0.5 kpc (see McMillan 2011; Sofue et al. 2009), and $6.2 \times 10^{10} M_{\odot}$ for NGC 4993 with the bulge of 1.5 kpc (see Lim et al. 2017), and the NFW halos masses are chosen as $9 \times 10^{11} M_{\odot}$ for the Milky Way with the concentration parameter of 6.5 and the scale radius of 32 kpc, and $2.3 \times 10^{12} M_{\odot}$ for NGC 4993 with the concentration parameter of 5.9 and the scale radius of 47.9 kpc. Because there is a typical uncertainty of 0.2 dex for the halo mass, the corresponding

parameters are also influenced for NGC 4993. In our calculations, we consider the maximum uncertainty of 0.2 dex and list them in Table 6. We can find if the halo mass of NGC 4993 changes from the maximum $10^{12.4}/hM_{\odot}$ to the minimum $10^{12.0}/hM_{\odot}$, the parameters (r_{200} , c_{200} , ρ_0 , R_s) for NFW halo change from (328 kpc, 5.6, $1.5 \times 10^{-3} M_{\odot} \text{pc}^{-3}$, 58 kpc) to (243 kpc, 6.2, $1.8 \times 10^{-3} M_{\odot} \text{pc}^{-3}$, 39 kpc). Thus there are some relatively small changes in the results listed in Table 5.

Secondly, the photons for comparison used in our calculation are considered as two cases, one is from GRB 170817A with short observed delay of 1.734 ± 0.054 s, and the other is from AT 2017gfo with long observation delay of 10.87 hour. The results obtained here suggest that the structure of two galaxies provides the big gravitational potentials and affects the comparison between various waves greatly. Therefore, the test of the WEP in BNS merger GW170817 is significantly enhanced. There are three points needed to be emphasized. (i) For the photons from GRB 170817A, the upper bound on PPN parameter difference of total potential is $|\Delta\gamma| \lesssim 10^{-9}$ which is justified by the result given by Wang et al. (2017), obtained by considering the potential fluctuations from the large scale structure and chosen a gravitational potential $\Phi \sim v_p R H_0 \sim 25\Phi_{MW}$. (ii) For the photons from AT 2017gfo, the result of total potential is $|\Delta\gamma| \lesssim 10^{-4}$ on the level of galaxy, which is looser by 2 orders of magnitude than the results $|\Delta\gamma| \lesssim 10^{-6}$ of the Virgo Cluster given by Wei et al. (2017) but on the level of cluster of galaxies. (iii) For the photons with the joint research group's emission assumption (see Abbott et al. 2017d), the result of total potential is in the range of $[-10^{-9}, 10^{-8}]$ which is significantly tighter by 2 orders of magnitude than that of $[-10^{-7}, 10^{-6}]$ given by Abbott et al. (2017d).

Thirdly, our calculation and analysis both show that the travelling waves are not only subject to the potential Φ_{mw} inside of the edge of local group (~ 1 Mpc), but are also governed by a large structure potential Φ_{host} in a more large range of [20 Mpc, 40 Mpc], which is illustrated in Figure 3. It suggests that if we consider a large scale gravitational potential the constraints on the WEP will be tighter than that of only by the measured Milky Way gravitational potential. This situation also could be found in other literature (e.g. Zhang 2016; Wang et al. 2017; Nusser 2016; Luo et al. 2016). Especially, Wang et al. (2017) presented two kinds of the WEP tests with/without considering the effects of a large structure in the Milky Way, and revealed there was a difference about 2 orders of magnitude between them. It should be noticed that in our calculation the luminosity distance to the source is adopted as the value of 40^{+8}_{-14} Mpc, which is the closest observed GWs source and the closest short γ -ray burst with a distance measurement (see Abbott et al. 2017a), but with a conservative uncertainty. We need to mention that several EM methods have given more precise values about the distance to the host galaxy, e.g. the distance of 40.4 ± 3.4 Mpc based on the MUSE/VLT measurement of the heliocentric redshift by Hjorth et al. (2017), the distance of 41.0 ± 3.1 Mpc by using HST measurements of the effective radius and the MUSE/VLT measurements of the velocity dispersion (see Hjorth et al. 2017), and the distance of $40.7 \pm 1.4 \pm 1.9$ Mpc by using surface brightness fluctuations by Cantiello et al. (2018) and so on.

In this paper, we choose the original value 40^{+8}_{-14} Mpc as a conservative distance to constrain the test of the WEP.

Fourthly, some observations show that there is an angle offset from the center of NGC 4993, corresponding to about 2 kpc offset at a 40 Mpc distance. It means that the transient could be located at any point along the line on sight in the galaxy of NGC 4993. Based on the observations from the HST and Chandra imaging (see Levan et al. 2017), they did not find any narrow interstellar medium features in the counterpart spectrum and could deduce the transient maybe locate at in front of the bulk of the host galaxy. Therefore the minimal distance of the source from the center of its host is just the projected distance, and its maximal distance is near the edge of NGC 4993. This kind of influence of angle offset on the results of PPN parameter difference could be quantified by the uncertainty of the line SN' in Figure 2. Through our calculations, we find that the values of SN' are about in the range of $[0, 13.06^{+0.09}_{-0.07}]$ kpc and the conservative relative deviation Δ is under 4×10^{-3} . Therefore, the uncertainty caused by the angle offset does not impact the orders of magnitude in our results, but it leads to some relatively small changes. The results for the maximum and the minimum SN' are listed in Table 4. This type of uncertainty from the transient could be eliminated by the further more accurate localization for the relative position to its host.

Finally, we need to point that in our calculation the BNS system is assumed conservatively to be inside or near the edge of NGC 4993. It is known that the natal kick imparted to the binary when the SN explosions that gave rise to the neutron stars. This kind of kick should lead to the mergers at large offsets from their birth sites and host galaxies, about tens to hundreds of kiloparsecs, in a broad range of merger timescales by Berger (2014). In Section 2.3 we choose a large NS kicks with V_{kick} of typical 400~500 km s^{-1} and check the uncertainty from it. The related delay time is adopted in a looser range from the observed minimal magnitude 86 Myr to the Hubble time. Through the quantitative estimation of the uncertainty, one can find that the large natal kicks does not effect the final results at the order of magnitude level, even for the Hubble time. For the tighter constraints on the delay time, one can refer to Figure 8 and Table 2 given by Abbott et al. (2017c) where the summary statistics for output PDFs and the more detailed PDFs on progenitor properties with various delay time constraints are presented.

ACKNOWLEDGEMENTS

We thank Dr. Jielei Zhang for helpful discussions. This work is supported by the National Natural Science Foundation of China under grants 11475143 and 11822304, and the Nanhu Scholars Program for Young Scholars of Xinyang Normal University.

REFERENCES

- Abbott B.P. et al., 2016, Phys. Rev. Lett., 116, 061102
- Abbott B.P. et al., 2017a, Phys. Rev. Lett., 119, 161101
- Abbott B.P. et al., 2017b, ApJ, 848, L12
- Abbott B.P. et al., 2017c, ApJ, 850, L40
- Abbott B.P. et al., 2017d, ApJ, 848, L13
- Arcavi I. et al., 2017, Nature, 551, 64

- Berger E., 2014, *ARA&A*, 52, 43.
- Breton R.P. et al., 2008, *Science*, 321, 104
- Cantiello M. et al., 2018, *ApJ*, 854, L31
- Connaughton V. et al., 2016, *ApJ*, 826, L6
- Coulter D.A. et al., 2017, *Science*, 358, 1556
- Duffy A.R. et al., 2008, *MNRAS*, 390, L64
- Ferdman R.D. et al., *ApJ*, 2013, 767, 85
- Gao H., Wu X.F., Meszaros P., 2015, *ApJ*, 810, 121
- Gillessen S. et al., 2009, *ApJ*, 692, 1075
- Goldstein A. et al., 2017, *ApJ*, 848, L14
- Haggard D. et al., 2017, *ApJ*, 848, L25
- Hernquist L., 1990, *ApJ*, 356, 359
- Hjorth J. et al., 2017, *ApJ*, 848, L31
- Huchra J.P. et al., 2012, *ApJS*, 199, 26
- Kafle P.R. et al., 2012, *ApJ*, 761, 98
- Kasliwal M. et al., 2017, *Science*, 358, 1559
- Kahya E.O., Desai S., 2016, *Phys. Lett. B* 756, 265
- Kramer M. et al., 2006, *Science*, 314, 97
- Krauss L.M., Tremaine S., 1988, *Phys. Rev. Lett.* 60, 176
- Lauberts A., Valentijn E.A., 1989, *European Southern Observatory*
- Levan A.J. et al., 2017, *ApJ*, 848, L28
- Lipunov V.M. et al., 2017, *ApJ*, 850, L1
- Lim S.H. et al., 2017, *MNRAS*, 470, 2982
- Liu M et al., 2017, *Phys. Lett. B*, 770, 8
- Longo M.J., 1988, *Phys. Rev. Lett.*, 60, 173
- Lu Y. et al., 2016, *ApJ*, 832, 39
- Luo Z.X. et al., 2016, *JHEA*, 9, 35
- McMillan P.J., *MNRAS*, 2011, 414, 2446
- Metzger B.D., Berger E., 2012, *ApJ*, 746, 48
- Misner C.W., Thorne K.S., Wheeler J.A., 1973, *Gravitation*, Freeman, San Francisco
- Nakar E., 2007, *Phys. Rept.*, 442, 166
- Navarro J.F., Frenk C.S., White S.D.M., 1996, *ApJ*, 462, 563
- Nusser A., 2016, *ApJ*, 821, L2
- Peters P.C., 1964, *Phys. Rev.*, 136, B1224
- Planck Collaboration, *A&A*, 2016, 594, A13
- Savchenko V. et al., 2017, *ApJ*, 848, L15
- Shapiro I.I., 1964, *Phys. Rev. Lett.*, 13, 789
- Soares-Santos M. et al, 2017, *ApJ*, 848, L16
- Sofue Y., Honma M., Omodaka T., 2009, *Publ. Astron. Soc. Japan*, 61, 227
- Tanvir N.R. et al., 2017, *ApJ*, 848, L27
- Tauris T.M. et al., 2017, *ApJ*, 846, 170
- Tingay S.J., Kaplan D.L., 2016, *ApJ*, 820, L31
- Wang H. et al., 2017, *ApJ*, 851, L18
- Wang Z.Y., Liu R.Y., Wang X.Y., 2016, *Phys. Rev. Lett.*, 116, 151101
- Wei J.J. et al., 2015, *Phys. Rev. Lett.*, 115, 261101
- Wei J.J. et al., 2016, *ApJ*, 818, L2
- Wei J.J. et al., 2017, *JCAP*, 11, 035
- Will C.M., 2014, *Living Rev. Relativ.*, 17, 4
- Will C.M., 2006, *Living Rev. Relativ.*, 9, 3
- Wu X.F. et al., 2016, *Phys. Rev. D* 94, 024061
- Yang X. et al., 2005, *MNRAS*, 356, 1293
- Yang S. et al., 2017, *ApJ*, 851, L48
- Zhang S.N., 2016, arXiv:1601.04558 [gr-qc].

This paper has been typeset from a $\text{\TeX}/\text{\LaTeX}$ file prepared by the author.